3rd URSI AT-AP-RASC, Gran Canaria, 29 May – 3 June 2022

Circular Polarization Antennas in Ridge Gap Waveguide at V-Band

Dayan Pérez-Quintana (1), (2), Iñigo Ederra (1), (2), and Miguel Beruete (1), (2)
(1) Department of Electrical, Electronic and Communications Engineering, Public University of Navarra, Spain
(2) Institute of Smart Cities (ISC), Public University of Navarra, Navarra, Spain

Abstract

In this paper, three compact antennas using the ridge gap waveguide (RGW) technology working in the millimeter-wave band (60 GHz) and generating circular polarization (CP) in either a wide or a narrow band are numerically and experimentally analyzed. The widest bandwidth achieved in CP is 14.48%, with respect to the central frequency and the highest gain is around 18.4 dB. These designs are a strong alternative for medium/high gain CP antennas in a planar layout covering different operation bandwidths for millimeter wave applications.

1. Introduction

The implementation of fifth-generation (5G) of mobile communications and the Internet of Things (IoT) is currently a fact. The high demand for faster speed and the increased volume of information required by these applications are impossible to satisfy with traditional operation bands at microwaves, as they do not have enough bandwidth. In addition, the constant growth of technology and communication systems has resulted in saturation of the lower part of the radio frequency spectrum which is a limited resource. Therefore, designing at higher frequencies rather than a solution is a necessity and will put antennas at the forefront as fundamental enabling devices. 5G is expected to entail a significant increase in bandwidth with high-frequency carriers, high density in connection stations, and a large number of antennas in each communication device. For these reasons, antennas working in wide frequency bands, compact and adaptable to any surface with the minimum possible loss is a key objective in this regard.

Recently, the 60 GHz frequency band has received increased interest and attention due to its potential functional benefits for many upcoming applications. A fundamental obstacle that must be circumvented to achieve a full development of high frequency technology is the problem of guiding waves with low loss. Traditional feeding systems like waveguides and microstrip lines suffer from increasing loss as the frequency grows. Using different feeding techniques can be a solution that, in combination with an appropriate fabrication method, could alleviate loss. In the last decade, Gap Waveguide (GW) technology (developed from the beginning by Prof. P.-S. Kildal) has gained a lot of interest since it is a reliable and competitive alternative for high-frequency communications [1]. Three main variants have been developed: Groove Gap Waveguide (GGW) [2], Ridge Gap Waveguide (RGW) [3] and Microstrip Gap Waveguide (MGW) [4] GW shows considerable improvements over traditional solutions like standard metallic waveguides, such as low loss, it does not require electric contact and it is easily adaptable to flat surfaces [5]-[9]. It also has a lower manufacturing cost with respect to traditional hollow waveguides, since the tolerances are coarser alleviating the fabrication constraints.

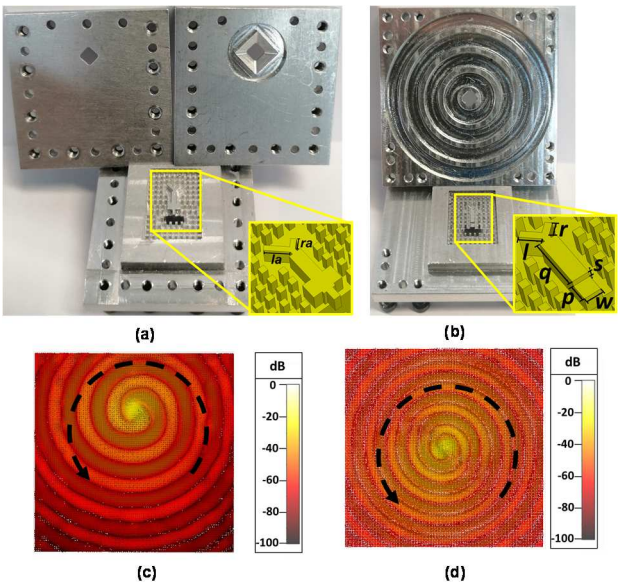

Figure 1. Photographs of (a) D and DHG antennas with the feeding system and (b) BE antenna. Main characteristics of antennas measured. Upper view of the surface current magnitude on: (c) D antenna and (d) BE antennas showing the rotation of currents in the RHCP direction.

Hence, the first objective of this investigation is to design antennas able to achieve good radiation characteristics and low losses using the RGW technique. In addition, all designs should be able to support the implementation of 5G mobile communications.

2. Antenna Designs

In this paper, we design, analyze and manufacture three antennas using Ridge Gap Waveguide (RGW) [1] technology, all of them with Circular Polarization (CP). The Transient Solver of the commercial simulator CST Microwave Studio® was used to simulate all the antennas. Photographs of the fabricated prototypes are shown in Fig. 1(a) and (b).

The structures are fed from the bottom by means of a standard WR-15 waveguide to make it compatible with standard measurement systems based on vector network analyzers. Three top plates were manufactured, each of them with a specific objective. The basic design is shown in Fig. 1(a) on the left, a diamond-shaped (D) slot antenna put on top of the feeding network plate. In addition, a circular groove concentric with the diamond slot is inserted for improving the gain of the antenna, Fig. 1(a) on the right. This last design is called diamond-horn-groove (DHG) antenna. Finally, a Bull's Eye antenna (BE) [10]-[13], shown in Fig. 1(b), with a narrow band but higher gain (Fig. 1(d)) culminates the objective of this investigation devoted to the development of compact millimeter wave CP antennas in RGW technology.

To generate the CP in these three antennas, two feeding systems were designed with different objectives. The insets of Figs. 1(a) and (b) show the particularities of both feeding systems. The first system designed, used for both D antenna and DHG antenna, is a stepped impedance matching network composed of three fundamental subsections to provide coupling from the WR-15 waveguide to RGW. Fig 1(b) down is the second feeding system designed specifically for BE antenna. The WR-15 to RGW transition consists of a simple step of height s = 0.38 mm and length p = 1.05 mm, as shown in Fig. 2(b). Although this feeder has a narrower axial ratio (AR) BW than the one used in [14], we opted for this solution because it is simpler, easier to fabricate and fits well with the requirements of BE antennas, which are usually narrowband. Both systems described have a good impedance matching as demonstrated in the back-to-back (i.e. two identical transitions connected back-to-back) simulation results in [10], [14].

Both feeding systems share the same way to generate CP; which is a feeding ridge terminated in two orthogonal arms of different lengths, inset of Fig. 1. This scheme guarantees in each case that the phase difference between both arms is close to 90º and the wave describes a spiral rotation achieving a CP field. However, the length difference between arms is not the same: in Fig. 1(a) the best AR was achieved with a difference around $\lambda_0/4$ (explained in detail in [14]); but due to the thickness increment of the BE antenna top plate the length between arms has to be reduced to $\lambda_0/10$ (explained in detail in [10]). The surface currents excited on the upper plates of the antennas have a clear spiral pattern, Fig. 1(c) and (d). Therefore, the combination of both elements (asymmetric arms and diamond slot shape) is able to generate CP in the systems. More specifically, the antenna supports right-handed CP (RHCP), with the current rotating in the right-handed direction.

3. Fabrication and Result Analysis

The material employed in all the structures is aluminum, due to its good conductivity in the operation band (σ_{Al} = 3.72×10^6 S/m), mechanical robustness and compatibility with standard manufacturing techniques. In addition, the antennas were manufactured using Standard Computer Numerical Control (CNC) milling machine method.

The experimental characterization was done in an anechoic chamber. A PNA network analyzer E8361C (Agilent Technologies) was used to measure the antennas, with the frequency span discretized in steps of 50 MHz. A single port calibration was performed to measure the reflection coefficient.

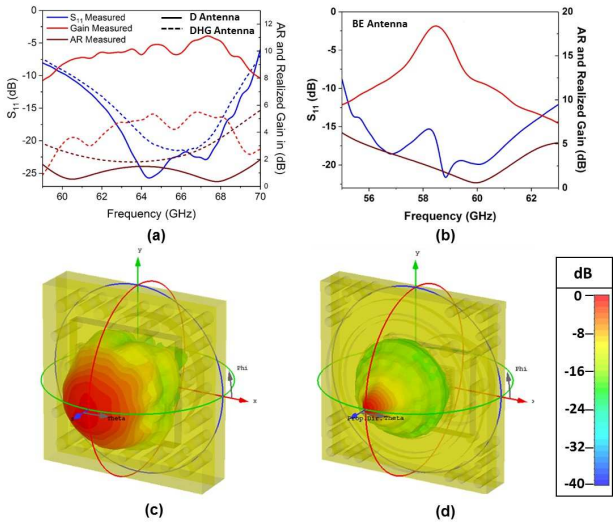

Figure 2. Main characteristics of antennas measured (a) D and DHG antennas. (b) BE antenna. Radiation patterns of (c) DHG antenna. (d) BE antenna.

The antenna performances were evaluated in terms of the reflection coefficient, broadside gain, axial ratio (AR) and polarization purity. Analyzing the experimental results, we note that the reflection coefficient in all the cases has good impedance matching, below −10 dB from 60.5 to 69.3 GHz, Fig. 4(a), and from 54.3 to 63.7 in the BE antenna shown in Fig 2(b) blue curve.

The characterization of the broadband gain was made by applying the gain transfer method. In all the cases, a sweep of $-90º \leq \theta \leq 90º$ was performed with a step of 0.5º, with a step of 50 MHz in each frequency range. Two different measurements were taken at each point by rotating the horn antenna (Mi-Wave 261) in two orthogonal positions. This is required because the test antenna has linear polarization and we need both orthogonal components to retrieve the CP response in the post-processing, which is based on the

method described in [15]. As shown in Fig. 2(a) red curve, the gain peak of the DHG antenna is 11.12 dB at 67 GHz in the experiment. Compared with the D antenna that has a maximum of 5.49 dB at 66.8 GHz Fig 2(a), this evolved design meets the intended objective of increasing the system gain. As a final evolution, the BE antenna achieves a peak gain around 18.4 dB at 58.5 GHz, Fig. 2(b) red curve, validating the idea of covering as much as possible the top area in order to maximize the gain. The gain decays away from the operation frequency, as typically happens in BE antennas. The aperture efficiency is approximately 9%, above the typical value of BE antennas.

The experimental AR is plotted in the solid brown curve of Fig. 2(a), (b). Taking as a criterion that the wave has CP when the AR is below 3 dB, we find that the CP BW is different in each design as we expected. Evidently, D and DHG antenna obtain a wide CP BW around 8 GHz (11.49%) and more than 9 GHz (17.32%) respectively, reaching the design objective. Fig 2(c) brown curve shows the AR of BE antenna. We find that the CP BW goes from 57.7 to 61.4 GHz and the minimum value (0.59 dB) is around 60 GHz. Fig. 2(c) and (d) show the three-dimensional radiation pattern where it can be notices them main lobe beamwidth difference among these designs.

Finally, Table I presents a comparison of our antennas with similar antennas reported in the literature, [3], [16], [17]. The structural characteristics and results achieved by each design are analyzed quantitatively. Note that most of these designs are antenna arrays, which are comparatively more complex than our antennas that are based on a single radiating element and a simple feeding network. In some cases, the antennas found in the literature have larger gain than the ones proposed here, so their bandwidth is restricted.

TABLE I
Comparison Between Different Millimeter-Wave Antennas

Ref	Number of Elements	Fractional BW (Total BW)*	Fractional BW (Total BW)$^{+}$	Peak Gain-(GBW)$^{\#}$
[3]	16 × 16	14% (57 - 66)	5.0% (59-62)	32.3 (96.9)
[16]	4 × 4	14.1 % (56 – 65)	21.1% (55-68)	19.5 (253.5)
[17]	2 × 2	18% (56 - 67)	16.7% (56–66.2)	14.6 148.9
D	1 × 1	14.24 % (60.5-69.3)	11.49% (59.9-67.2)	11.12 (122.3)
DHG	1 × 1	14.64 % (60.3-69.6)	17.32% (60-71)	11.12 (122.3)
BE	1 × 1	16.16 % (54.3 – 63.7)	6.3% (57.7 - 61.4)	18.4 (68.0)

*Defined as S11 < −10 dB. Total BW is in GHz
$^{+}$Defined as AR < 3 dB. Total BW is in GHz
$^{\#}$Peak Gain is in dB. For the gain-bandwidth product (GBW) calculation, the BW is defined as AR < 3 dB

4. CONCLUSIONS

To sum up, in this article, we have designed three antennas with CP operating in the V-band of millimeter waves based on RGW technology. The CP generation mechanism is based on the length difference between two orthogonal arms at the end of the ridge. The feeding system allows the generation of CP in a simple way, without the need of implementing an array along with a complex feeding network. Several changes were done in order to improve the gain, being the most important one the design of a BE structure consisting of four concentric periodic corrugations around the slot to enhance the gain by covering maximally the top metallic plane. The experimental results demonstrate good radiation characteristics with a compact and low profile structure. A high gain of around 18.4 dB at 58.5 GHz is achieved by the BE antenna and a CP BW of 14.48 % with respect to the center frequency by the DHG antenna, being these the most relevant results. In addition, all the antennas have RHCP with more than 30 dB of cross-polarization isolation in the BE case. In comparison with similar antennas, our designs are competitive variants that can have different uses, either in the imminent implementation of the 5G, IoT, or in any application that is supported in the 60–70 GHz band.

5. Acknowledgements

Project RTI2018-094475-B-I00 funded by MCIN/ AEI /10.13039/501100011033/ FEDER “Una manera de hacer Europa”

References

[1] M. A. Al-Absi, A. A. Al-Absi, M. Sain, and H. J. Lee, “A State of the Art: Future Possibility of 5G with IoT and Other Challenges,” 2020, pp. 35–65.
[2] P.-S. Kildal, E. Alfonso, A. Valero-Nogueira, and E. Rajo-Iglesias, “Local Metamaterial-Based Waveguides in Gaps Between Parallel Metal Plates,” IEEE Antennas Wirel. Propag. Lett., vol. 8, pp. 84–87, 2009.
[3] M. Ferrando-Rocher, A. Valero-Nogueira, J. I. Herranz-Herruzo, and J. Teniente, “60 GHz Single-Layer Slot-Array Antenna Fed by Groove Gap Waveguide,” IEEE Antennas Wirel. Propag. Lett., vol. 18, no. 5, pp. 846–850, May 2019.
[4] A. U. Zaman and P. Kildal, “Wide-Band Slot Antenna Arrays With Single-Layer Corporate-Feed Network in Ridge Gap Waveguide Technology,” IEEE Trans. Antennas Propag., vol. 62, no. 6, pp. 2992–3001, 2014.
[5] T. Manabe et al., “Polarization dependence of multipath propagation and high-speed transmission characteristics of indoor millimeter-wave channel at 60 GHz,” IEEE Trans. Veh. Technol., vol. 44, no. 2, pp. 268–274, May 1995.
[6] J. Hirokawa and M. Zhang, Handbook of Antenna Technologies. Singapore: Springer Singapore, 2014.
[7] J. Xi, B. Cao, H. Wang, and Y. Huang, “A novel 77 GHz circular polarization slot antenna using ridge gap

waveguide technology," in 2015 Asia-Pacific Microwave Conference (APMC), 2015, pp. 1–3.
[8] T. Li and F. Fan, "Design of ka-band 2×2 circular polarization slot antenna array fed by ridge gap waveguide," in 2017 Sixth Asia-Pacific Conference on Antennas and Propagation (APCAP), 2017, pp. 1–3.
[9] M. Ferrando-Rocher, J. I. Herranz-Herruzo, A. Valero-Nogueira, and A. Vila-Jimenez, "Single-Layer Circularly-Polarized Ka-Band Antenna Using Gap Waveguide Technology," IEEE Trans. Antennas Propag., vol. 66, no. 8, pp. 3837–3845, Aug. 2018.
[10] D. Perez-Quintana, I. Ederra, and M. Beruete, "Bull's-Eye Antenna with Circular Polarization at Millimeter Waves based on Ridge Gap Waveguide Technology," IEEE Trans. Antennas Propag., no. c, pp. 1–1, 2020.
[11] M. Beruete et al., "Very low-profile 'Bull's Eye' feeder antenna," IEEE Antennas Wirel. Propag. Lett., vol. 4, no. 1, pp. 365–368, 2005.
[12] A. A. Oliner, "Leaky-Wave Antennas," in Antenna Engineering Handbook, R. C. Johnson, Ed. New York: Mc Graw-Hill, 1993.
[13] M. Guglielmi and D. R. Jackson, "Broadside radiation from periodic leaky-wave antennas," IEEE Trans. Antennas Propag., vol. 41, no. 1, pp. 31–37, 1993.
[14] D. Perez-Quintana, A. Torres-Garcia, I. Ederra, and M. Beruete, "Compact Groove Diamond Antenna in Gap Waveguide Technology with Broadband Circular Polarization at Millimeter Waves," IEEE Trans. Antennas Propag., pp. 1–1, 2020.
[15] Bee Yen Toh, R. Cahill, and V. F. Fusco, "Understanding and measuring circular polarization," IEEE Trans. Educ., vol. 46, no. 3, pp. 313–318, Aug. 2003.
[16] T. H. Jang, Y. H. Han, J. Kim, and C. S. Park, "60 GHz Wideband Low-Profile Circularly Polarized Patch Antenna With an Asymmetric Inset," IEEE Antennas Wirel. Propag. Lett., vol. 19, no. 1, pp. 44–48, Jan. 2020.
[17] Q. Zhu, K. B. Ng, and C. H. Chan, "Printed circularly polarized open loop antenna array for millimeter-wave applications," in 2017 IEEE International Symposium on Antennas and Propagation & USNC/URSI National Radio Science Meeting, 2017, vol. 2017–Janua, no. 2, pp. 2561–2562.